



# Designing Detectors for RF/ID Tags

## Application Note 1089

### Abstract

The RF/ID market is growing rapidly, with everything from cattle to cars carrying radio frequency identification (RF/ID) tags. Severe cost, size and DC power constraints in the tag itself have forced designers to abandon superheterodyne receivers for the older and simpler crystal video receiver. Consisting of a simple detector circuit and a printed antenna, this receiver can be built for pennies. This paper will describe two zero bias detector circuits for such applications, one operating at 915 MHz and the other at 2.45 GHz. Design equations for diode selection will be given, as well as techniques for the realization of practical impedance matching networks. Measured performance, taken from prototype detectors, will be presented.

### Introduction

Bar codes have become ubiquitous in our society. They permit the swift and accurate identification of material in every venue from supermarket to warehouse. However, they suffer from some limitations. Most importantly, their range is limited to inches and they require a clean and rela-

tively benign environment in order to operate reliably.

The RF/ID tag is the logical next step from the bar code identification system. A RF interrogator replaces the bar code reader. A small and low cost RF transponder, or tag, replaces the bar code marking. Depending upon the frequency of operation (120 kHz, 915 MHz, 2.45 GHz and 5.8 GHz are common) and the exact kind of tag design, such RF/ID tags and

their interrogators can offer operating ranges of tens of meters and they operate successfully in dirty or hostile environments. Such RF/ID systems are being successfully used to remotely identify and track cattle, household pets, automobiles passing through toll booths, supermarket carts, cocktail waitresses, truck tires, railroad cars, personnel entering and leaving secure facilities and others.

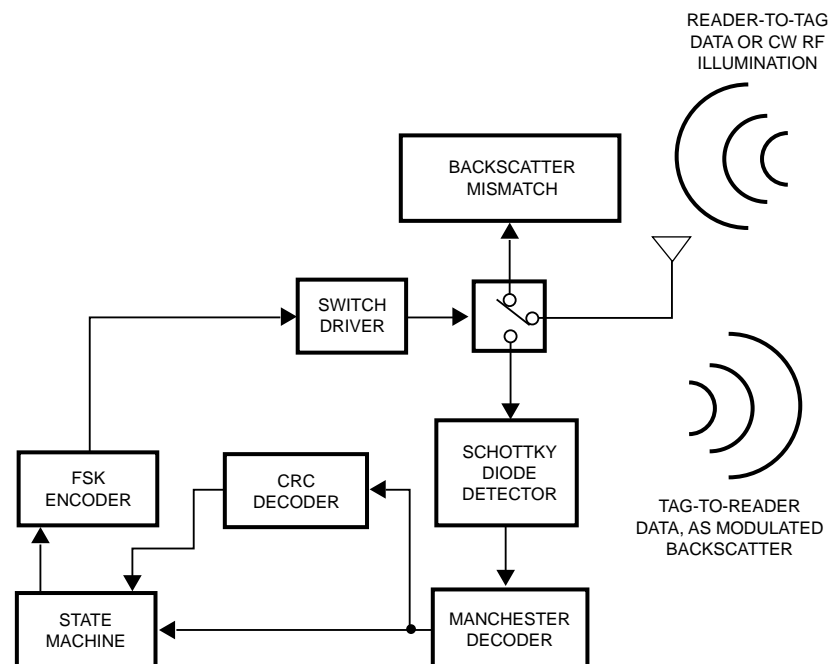


Figure 1a. Typical RF/ID Tag Block Diagram (tag)

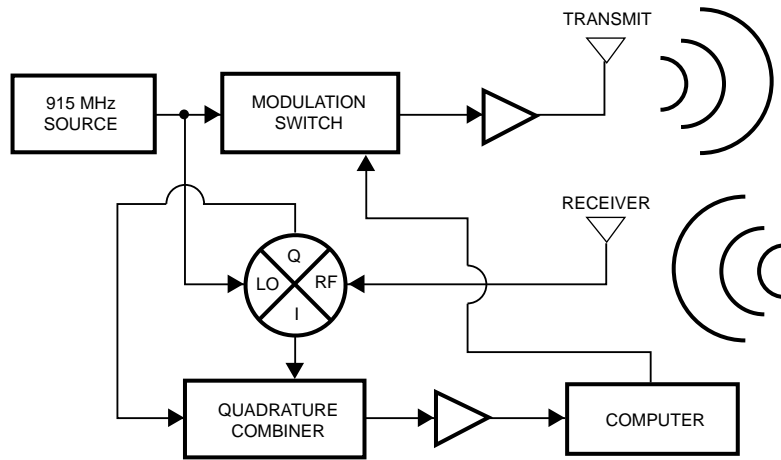


Figure 1b. Typical RF/ID Tag Block Diagram (reader)

A typical RF/ID system has relatively few interrogators and many tags. Thus, the most severe design constraints are placed on the portable transponder, or tag. These are:

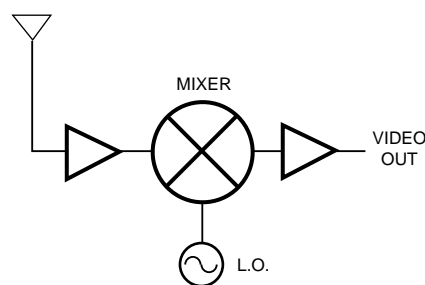
**Small size:** The tag used to RF/ID household pets is surgically implanted just below the animal's skin — size is obviously critical. An automotive toll tag, placed in a car's windshield, is limited in size.

**Low cost:** In order to be commercially successful, the tag itself must be very low in cost.

Some tags are active, having an on-board transmitter with which to reply to the interrogator, while others are passive and operate (as shall be seen below) without a transmitter. Some tags have a simple memory, programmed at the factory and consisting of no more than a unique serial number, while others have more elaborate

READ/WRITE memories which enable them to store information for later retrieval. What they all have in common is the need for a low cost, compact receiver. A typical RF/ID tag block diagram<sup>(1)</sup> is shown in Figure 1, along with its associated reader — this is the type of tag being adopted for the CalTrans (California Department of Transportation) electronic toll payment system on the bridges of the San Francisco bay area.

In this system, the reader or interrogator sends a modulated RF signal which is received by the tag. The Schottky diode detector demodulates the signal and sends the data on to the digital circuits of the tag — this is the so-called



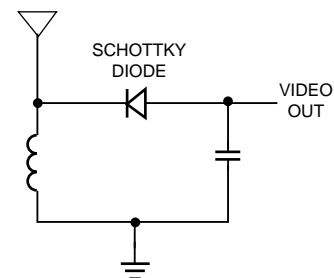
SUPERHETERODYNE RECEIVER

“wake up” signal. The reader stops sending modulated data and illuminates the tag with a continuous wave (CW) or unmodulated signal. The tag's FSK encoder and switch driver switch the load placed on the tag's antenna from one state to another, causing the radar cross-section of the tag to be changed. As a result, the weak signal reflected from the tag is modulated — this signal is then detected by the reader's receiver. In this way, the reader and the tag can communicate using RF generated only in the reader, eliminating the need for the tag to have its own transmitter. For more detail on the operation of this system, see reference (1).

## Receiver Types

The superheterodyne receiver is contrasted with the crystal video receiver in Figure 2.

The superhet receiver offers typical sensitivity greater than -150 dBm, thanks to the RF and video low noise amplifiers which are part of the circuit. The crystal video receiver, identical to the crystal radio with which many of us experimented in our youth, is limited in its sensitivity to something on the order of -55 dBm. However, the crystal video receiver consists of no more than a diode, a capacitor, and a choke —



CRYSTAL VIDEO RECEIVER

(1) Lawrence Livermore Labs, *An Automatic Vehicle ID System for Toll Collecting*, Lawrence Livermore National Laboratory LLNL Transportation Program, L-644

Figure 2. Receiver Block Diagrams

it can be built (in high volume) for pennies. The superhet receiver is a complex collection of ICs and discrete components necessary to realize its frequency mixer, amplifiers and RF oscillator. Cost and size considerations have driven the RF/ID industry to adopt the crystal video receiver for the tag itself, using the superhet only in the interrogator.

### Detector Circuits

A typical RF/ID tag receiver can be divided into the antenna and the detector circuit<sup>(2)</sup>. The antenna is a printed patch or dipole, an integral part of the circuit board on which the receiver is realized. The detector circuit itself is broken down into three blocks in Figure 3.

The RF impedance matching network is vital to obtaining the best performance possible from a given diode circuit. The design of it is described in detail in a following section.

The diode circuit can take many forms, depending upon the demands of a specific design — four of them are shown in Figure 4.

Single diode circuits offer simplicity and minimum cost as their advantage, and they are the most common type. The voltage doubler produces a higher output for a given input power and offers a lower input impedance to the source, simplifying the input impedance matching network. Either can be realized using conventional or zero bias Schottky diodes. Diode characteristics are described in greater detail in a following section.

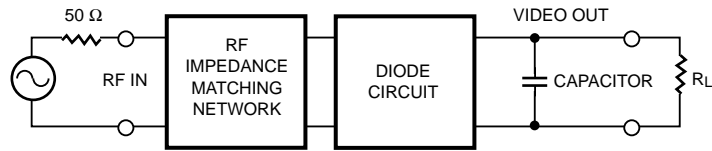


Figure 3. Block Diagram of a Detector Circuit

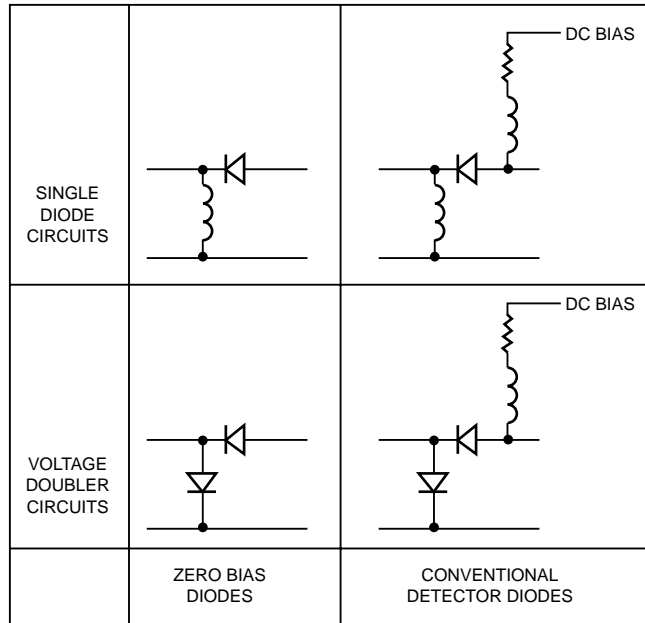


Figure 4. Common Types of Diode Circuits

Finally, the capacitor shown in Figure 3 separates the RF from the video sides of the circuit. It can be either lumped (as a chip soldered to the PC board) or distributed (as a patch etched into the circuit). It must provide a good RF short circuit to the diode, to insure that all of the RF voltage appears across the diode terminals. However, it must be small at video frequencies, so that it does not load down the video circuit.

### Diode Basics

The job of the detector diode is to convert input RF power to output voltage. A typical transfer curve for a Schottky detector diode is shown in Figure 5.

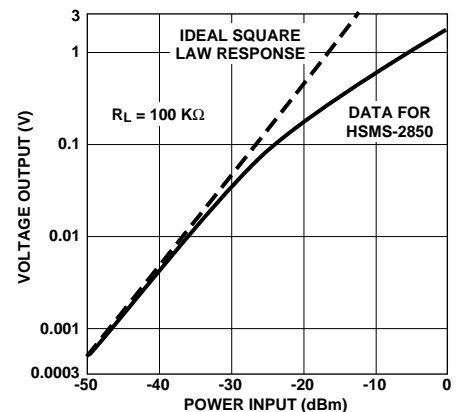


Figure 5. Typical Detector Transfer Curve

At low power levels, the transfer characteristic of a Schottky diode follows a square-law rule, with voltage output proportional to power (voltage squared) input. As input power is increased, the

(2) Agilent Technologies Application Note 923, *Schottky Barrier Diode Video Detectors*.

slope of the  $V_o/P_{in}$  curve flattens out to more nearly approximate a linear (voltage output proportional to RF voltage input) response. Methods have been developed to extend the square law range (3),(4), but they are not of interest in the design of RF/ID tags. From Figure 5, it can be seen that the key performance parameter for a detector diode operating in the square law region is voltage sensitivity, generally referred to as  $\gamma$  and expressed in millivolts/microwatt. Since the diode's transfer characteristic deviates from square law at relatively low power levels (see Figure 5), this number is generally specified at -30 or -40 dBm.

At small signal levels, the Schottky diode can be represented by a linear equivalent circuit, as shown in Figure 6.

$R_j$  is the junction resistance (sometimes referred to as  $R_v$ , or video resistance) of the diode, where RF power is converted into video voltage output. For maximum output, all the incoming RF voltage should ideally appear across  $R_j$ .  $C_j$  is the junction capacitance of the diode chip itself. It is a parasitic element which shorts out the junction resistance, shunting RF energy to the series resistance  $R_s$ .  $R_s$  is a parasitic resistance representing losses in the diode's

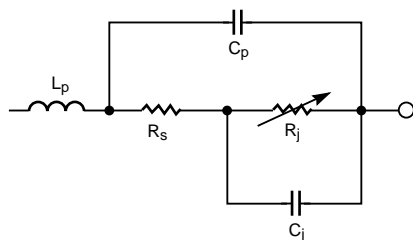


**Figure 6. Equivalent Circuit of a Schottky Diode**

bondwire, the bulk silicon at the base of the chip and other loss mechanisms. RF voltage appearing across  $R_s$  results in power lost as heat.  $L_p$  and  $C_p$  are package parasitic inductance and capacitance, respectively. Unlike the two chip parasitics, they can easily be tuned out with an external impedance matching network.

The equation for junction resistance at 25°C is:

$$R_j = 0.026 / I_T \quad (1)$$

where

$I_T = I_s + I_b$  in amperes

$I_s$  = the diode's saturation current, a function of barrier height

$I_b$  = externally applied bias current

Given a knowledge of the package parasitics  $L_p$  and  $C_p$ , the chip parasitics  $R_s$  and  $C_j$ , the diode's saturation current  $I_s$ , and the video load resistance  $R_L$ , one can calculate the voltage sensitivity of a Schottky diode. It can be shown(5) that the expression for sensitivity, assuming a perfect, lossless impedance match at the diode's input, is

$$\gamma_2 = \frac{0.52}{I_T (1 + \omega^2 C_j^2 R_s R_j) (1 + R_j/R_L)} \quad (2)$$

where

$C_j$  = junction capacitance in farads

$R_L$ ,  $R_s$ , and  $R_j$  are in ohms

From equation (2), one can see that the video load resistance  $R_L$  must be large compared to the diode's junction resistance  $R_j$ . The former is often set to 100 K $\Omega$  or higher, but the designer does not always have control over it.  $R_j$  can, of course, be lowered

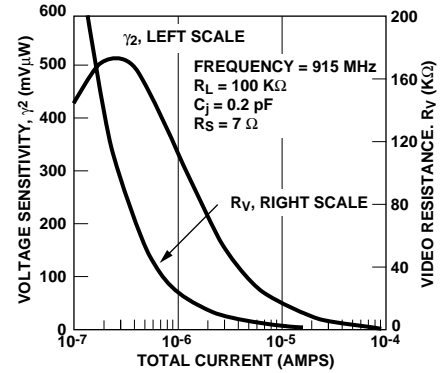


**Figure 7.  $\gamma_2$  as a function of  $I_T$**

through an increase in DC bias current  $I_b$  (if it is available). However, since  $I_T$  appears in the denominator of equation (2), raising bias current too high can reduce  $\gamma_2$ . See Figure 7.

In this figure, the tradeoff between sensitivity and junction resistance is clearly shown. For this n-type diode operating at 915 MHz, a choice of 0.3  $\mu$ A total DC current will result in the maximum value of sensitivity but with  $R_j = 90$  K $\Omega$ . As shall be seen in the following sections, an impedance of 90 K $\Omega$  cannot be matched to 50  $\Omega$ , so this high level of sensitivity is unavailable in a practical circuit design. Because of impedance matching limitations, a total operating current of 2.5 to 25  $\mu$ A is usually chosen for R.F. detectors.

Also from equation (2), it can be seen that  $C_j$  and  $R_s$  must be minimized in order to obtain the maximum value of  $\gamma_2$ . Unfortu-

(3) Agilent Technologies Application Note 986, *Square Law and Linear Detection*.

(4) Agilent Technologies Application Note 956-5, *Dynamic Range Extension of Schottky Detectors*.

(5) Agilent Technologies Application Note 969, *The Zero Bias Schottky Detector Diode* (revised 8/94).

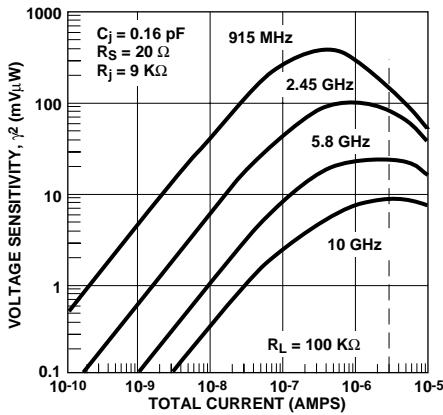


**Figure 8. Calculated Values of  $\gamma^2$  for a Typical Diode**

nately, in the design of Schottky diodes, a change (such as reducing contact diameter) which reduces  $C_j$  will increase  $R_s$ . Obviously, the effect of  $C_j$  will be more significant in a detector operating in X-Band, while  $R_s$  will be the important parasitic for a detector operating in the tens of MHz. One can use a spreadsheet program to produce a plot of equation (2) for a typical detector diode, as shown in Figure 8.

This figure shows the calculated voltage sensitivity for the Agilent Technologies HSMS-2850 zero bias Schottky (or any other diode having the same  $R_j$ ,  $R_s$ , and  $C_j$ ) at four frequencies. The effect of junction capacitance can be seen in the fact that  $\gamma$  is lower at higher frequencies. It can also be seen that the peak sensitivity occurs at different values of  $I_T$  for different frequencies. The vertical line on the plot marks the saturation current for this diode — it is the operating current in zero bias applications.

The designer is faced with the choice of two kinds of Schottky diodes for RF/ID applications, the externally-biased and the zero bias diode.

Externally-biased diodes are typically formed on n-type silicon with medium and high barrier metal systems, which offer a lower value of  $R_s$ , for a given value of  $C_j$ . Since their typical saturation currents are in the range of nanoamperes, they must have external bias in order to operate at small signals. Zero bias diodes, on the other hand, are low barrier Schottky devices formed on p-type silicon. Through the careful choice of barrier height, saturation currents in the range of 1 to 10  $\mu$ A are achievable.

Besides differing in their R-C constant, n-type and p-type Schottky diodes exhibit different values of flicker noise (6) at low frequencies. Flicker noise is that excess noise which occurs at very low frequencies, as shown in Figure 9.

Flicker noise is generated at the rim of the Schottky contact, where metal, silicon and passivation meet. It can be minimized by eliminating the passivation, but such diodes have poor reliability when put in low-cost plastic packages. The HSMS-8101 is a passivated n-type diode, suitable for use in mixers and DC biased detectors. Note that increasing the bias current lowers the junction resistance, which (in turn) reduces the asymptotic value of flicker noise voltage. However, as described in reference (6), the flicker noise of the p-type HSMS-2850 at zero bias is superior at low frequencies. RF/ID tags often have data rates in the range of 100 Hz to 10 kHz, where excessive low frequency flicker noise in the diode can reduce sensitivity.

Each diode type has its advantages. The n-type diode offers the lowest possible  $R_s$  and thus the

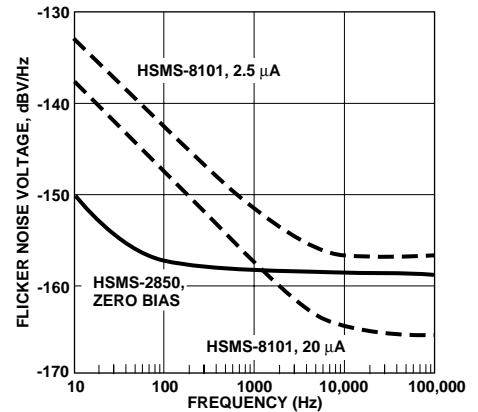


**Figure 9. Typical Flicker Noise in Schottky Diodes**

highest value of  $\gamma$ . The designer can use a matched pair (the second diode providing a voltage reference) with an op amp to obtain good temperature stability. Finally, through the control of DC bias, the designer can obtain high video bandwidth with a DC biased diode.

The p-type, on the other hand, offers the lowest possible cost, size and complexity in that it does not require DC bias, and it exhibits the lowest flicker noise. It is for these reasons that the zero bias Schottky is the diode of choice for RF tag applications.

### Impedance Matching Networks – The Ideal (lossless) Case

A complete treatment on RF impedance matching networks can be found elsewhere (7). Matching the impedance of a Schottky diode over a wide (octave or greater) bandwidth can present a challenge to the designer (8). How-

(6) Agilent Technologies Application Note 956-3, *Flicker Noise in Schottky Diodes*.

(7) Agilent Technologies Application Note 963, *Impedance Matching Techniques for Mixers and Detectors*.

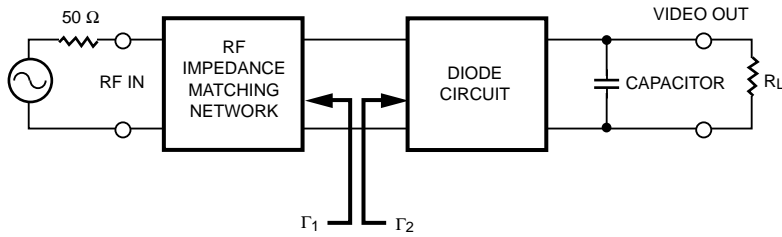


**Figure 10. Impedance Matching Requirement**

ever, a general design approach for narrow (less than 10%) bandwidths is straightforward.

Consider the detector circuit shown in Figure 10. At any frequency and input power level, the diode will have an input reflection coefficient  $\Gamma_2$ , with magnitude  $\rho_2$  and angle  $\theta_2$ . In order to achieve a perfect impedance match (and, thus, maximum power transfer) at a given frequency, one must set  $\Gamma_1$  to be the complex conjugate of  $\Gamma_2$ , which is to say that two conditions must be satisfied:

$$\rho_1 = \rho_2$$

$$\theta_1 = -\theta_2 \quad (3)$$

For most tag applications, cost is an overriding consideration. Plastic packages such as the SOT-23 offer the lowest cost (lower even than the unpackaged chip diode) and are thus the package of choice. Referring to Figure 6, the package parasitics for a SOT-23 are:

$$L_p = 2.0 \text{ nH}$$

$$C_p = 0.08 \text{ pF}$$

For a state-of-the-art zero bias Schottky such as the Agilent Technologies HSMS-2850, the chip characteristics are

$$R_s = 20 \text{ } \Omega$$

$$C_j = 0.16 \text{ pF}$$

$$I_s = 3 \text{ } \mu\text{A (or, } R_j = 9 \text{ K}\Omega)$$

Using the equivalent circuit of Figure 6 and these values, one can obtain the diode reflection coefficient shown in Figure 11 through the use of a linear analysis program such as MMICAD (9). Such an equivalent circuit is sufficiently accurate for design work to frequencies of 6 GHz or higher.

A two-element impedance matching network, as shown in Figure 12, is sufficient to match the diode to 50  $\Omega$  at any single frequency.

Consider  $\Gamma_2$ , the diode's reflection coefficient at 915 MHz, shown as point **A** in Figure 13. The addition of a series matching reactance  $X_1$  (consisting of a combination of lumped inductance and microstrip transmission line) rotates the diode's impedance around to point **B** on the line of constant conductance shown as a dashed line in Figure 13. The addition of a shunt reactance  $X_2$ , brings the input characteristic to point **C** (a perfect impedance match).  $X_2$  can

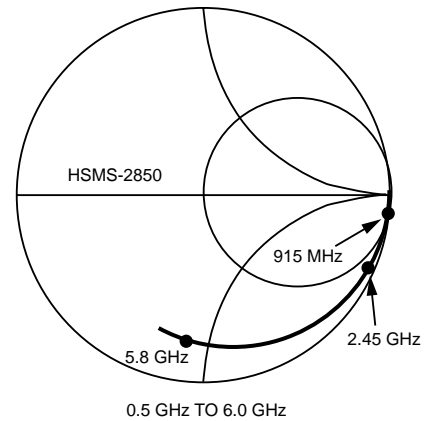


**Figure 11.  $\Gamma_2$ , Input Reflection Coefficient, HSMS-2850**

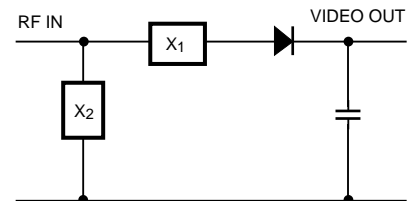


**Figure 12. Ideal Matching Network**

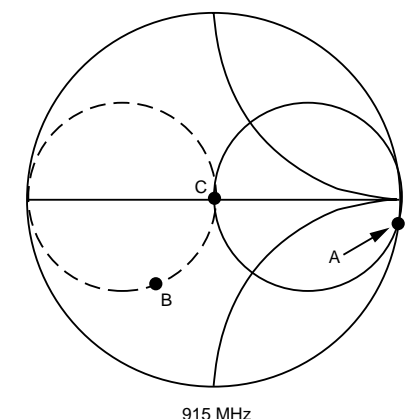
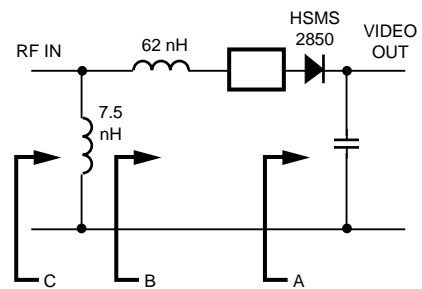


**Figure 13. 915 MHz Impedance Transformation**

(8) R.W. Waugh, J.A. Garcia and D.L. Lacombe, "Designing Limiter/Detectors for ECM Receivers," *Microwaves*, Vol. 11, No. 10, October, 1972

(9) Product of Optotek Limited, 62 Steacie Drive, Kanata, Ontario, Canada K2K 2A9

be realized either as a lumped inductor or as a shorted transmission line of length  $< \lambda/4$ . This element serves not only to complete the impedance matching task, but it also serves as a current return for the diode.

To this point, the discussion has assumed a source impedance of  $50 + j0 \Omega$ . However, in RF/ID tags, the diode's source is the antenna. While it is possible to match the antenna to  $50 \Omega$  and then match the diode to the same impedance, improved performance and smaller size will be achieved by minimizing the number of impedance matching elements. If the diode is moved very close to the antenna, a single impedance transformer can be used to match the diode's impedance to that of the antenna. Moreover, if the antenna's impedance is in the upper half of the Smith Chart, close to a complex conjugate of the diode's impedance, the task of impedance transformation will be made easier and transformer losses (discussed in the next section) will be minimized. For example, if the antenna impedance is  $50 + j50 \Omega$ , the matching network's source impedance is closer to the complex conjugate of the diode impedance, as seen in Figure 14 — the matching network will be easier to design and lower in loss than one matching the diode to  $Z_0 = 50 + j0$ .

Obviously, an easier impedance transformation is the result.

This, then, is the general approach used to realize the impedance matching network at the input to the Schottky diode. However, some practical considerations must be taken into account.

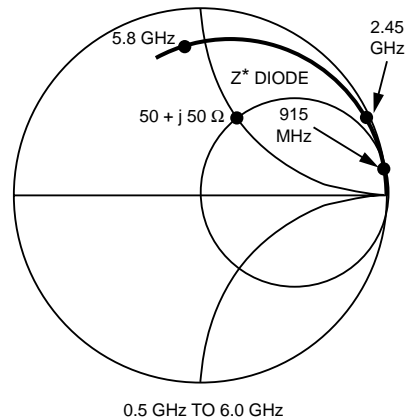


**Figure 14.**  $\Gamma_2^*$  for HSMS-2850 compared to  $Z = 50 + j50$

### Impedance Matching Networks – The Real World

Reference (5) defines  $\gamma_2$  as the voltage sensitivity of a detector diode having a perfect, lossless impedance match to the RF source (which is assumed to be  $50 \Omega$  in the general case). If such an ideal matching network could be realized as described in Figure 12, a typical detector diode would produce the voltage sensitivity shown in Figure 7. At a total bias current of  $0.3 \mu\text{A}$ , such a diode could be expected to produce more than  $500 \text{ mV}/\mu\text{W}$  into a  $100 \text{ k} \Omega$  load at  $915 \text{ MHz}$ .

At RF and microwave frequencies, lumped inductors and transformers exhibit Q values of 30 to 80. Lumped capacitors offer a wider range, from 10 to 500, depending upon the type of construction. Distributed-element matching networks suffer from conductor losses and, especially in FR4, in dielectric losses. To take these losses into account,  $\gamma_3$  is defined as the actual voltage sensitivity achieved with a practical matching network.

$$\gamma_3 = \gamma_2 (\text{LF}) \quad (4)$$

where LF is a loss factor to be defined below.

Consider the diode equivalent circuit shown in Figure 6. Four of the five elements are fixed for a given diode and package — only  $R_j$  is a (current-controlled) variable (10). Using the values of these four fixed circuit elements and the relation for  $R_j$  as a function of  $I_T$  given in equation (1) and plotted in Figure 7, one can compute the input reflection coefficient  $\Gamma_2$  of the diode as a function of frequency and total current. The result will be a family of curves such as the one shown in Figure 11.

A thorough discussion of losses in lumped and distributed-element matching networks is beyond the scope of this paper. However, the designer can consider the generalized matching network shown in Figure 15.

Working out from the load (the diode), the first element is a lossless transmission line. This line has a characteristic impedance equal to the impedance of the diode and is of sufficient negative length to rotate the diode's

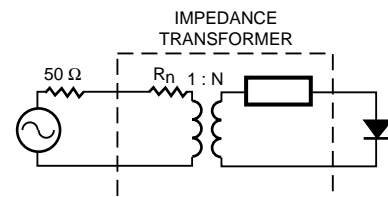


**Figure 15.** Generalized Matching Network

(10) This is actually an approximation, since  $C_j$  is also a function of forward current. However, the error introduced by this approximation is small.

impedance back up to the real axis of the Smith chart. The second element of the network is an ideal 1:N transformer. It can be shown that the turns ratio is given by:

$$N = \left( \frac{1 + \rho}{1 - \rho} \right)^{0.5} \quad (5)$$

where  $\rho$  = the magnitude of the diode's reflection coefficient.

This transformer matches the diode's impedance to the source impedance (the center of the Smith Chart).

The third element of the network is a series resistor,  $R_n$ , representing the losses in the network.

This general network, then, can be used to provide a lossy match of the diode to a  $50 \Omega$  source (11). It can be shown that, when  $N$  and the length of the transmission line are adjusted to provide a perfect match to the source, the loss factor of the network is given by:

$$LF = \left( \frac{1}{1 + \frac{KNX}{100}} \right)^2 \quad (6)$$

where  $X$  and  $K$  are empirically derived constants and the loss factor is given as a power ratio (12).

In lumped element transformers(13), the value of  $X$  falls between 1 and 3. For circuits realized using lumped or distributed elements on FR4 at frequencies from 1 to 6 GHz, the author has obtained good agreement between computed and measured values of  $\gamma_3$  using:

$$\begin{aligned} X &= 2.2 \\ K &= 0.35 \end{aligned}$$

An examination of equations (5) and (6) reveals that the losses are strongly dependent upon  $\rho$ , the magnitude of the diode's reflection coefficient, and upon the resulting turns ratio,  $N$ .  $\rho$  is a function of  $R_j$ , which is, in turn, a function of the total current flowing through the diode. As  $I_T$  is increased,  $R_j$  is lowered,  $\rho$  drops, and the losses of the practical matching network go down.

By applying equation (4) to the  $\gamma_2$  data plotted in Figure 7,  $\gamma_3$  can be calculated for a typical diode with a practical RF impedance matching network:

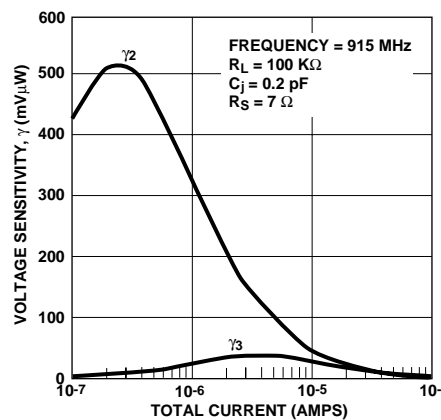


Figure 16.  $\gamma_3$  and  $\gamma_2$  as a function of  $I_T$

The impact of matching network losses are dramatic at this frequency. The scale of the curve is expanded in Figure 17.

Not only is the peak sensitivity available from our typical diode reduced from 500 to 40 mV/ $\mu$ W, but the peak shifts from  $I_T = 0.3 \mu$ A to  $3 \mu$ A.

Of course, the use of a high quality silver-plated tuner to match the diode to  $50 \Omega$  will result in lower losses and higher sensitivity, but such tuners are much too

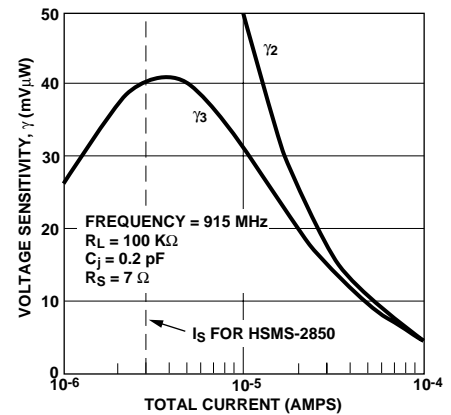


Figure 17. Expanded Scale

bulky and expensive for RF/ID tags.

In Figure 8,  $\gamma_2$  vs. frequency was examined for the HSMS-2850 zero bias Schottky. This same analysis can be performed on that diode to produce the following figure.

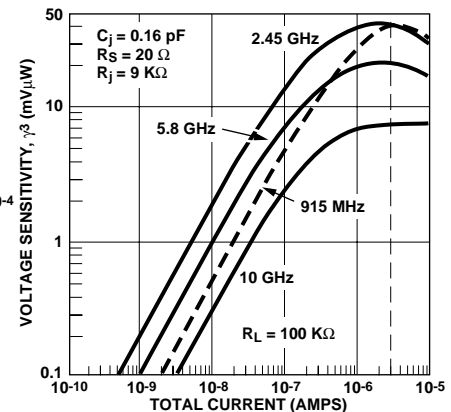


Figure 18. Calculated values of  $\gamma_3$  for the HSMS-2850

(11) Provided that  $R_n$  is small compared to  $50 \Omega$ . For large values of  $R_n$ , some impedance mismatch will occur, and the ratio  $N$  of the transformer will have to be adjusted accordingly.

(12) This paper deals with square law detectors, in which the output voltage varies as the input power.

(13) *Reference Data for Engineers: Radio, Electronics, Computer, and Communications*, Sams Publishing, Carmel, Indiana, 1985, pp. 13-27 – 13-29.



In this figure, total current is shown as the independent variable, but the actual saturation current of the HSMS-2850 is shown as the vertical dashed line. Comparing this figure to Figure 8, one can see that practical matching networks reduce the available sensitivity by an order of magnitude. Further, it can be seen that the  $3 \mu\text{A}$  saturation current of this zero bias Schottky was carefully chosen to produce the maximum sensitivity in practical RF/ID tag applications.

Thus, given the values for operating frequency and video load resistance (and external bias current, if it is available), as well as the diode characteristics  $I_s$ ,  $R_s$ , and  $C_j$ , the designer can use equations (2) and (4) to estimate the value of voltage sensitivity he will obtain from a Schottky detector to a high degree of accuracy.

It should be noted that if the RF source is an antenna having an impedance in the upper half of the Smith chart (see Figure 14, above), the value of the diode's  $\rho$  will be reduced compared to this source impedance and matching network losses can be substantially reduced.

### Examples

Two circuits were fabricated and tested to illustrate the methods described above. The first was a detector using a single diode and operating at the 2.45 GHz frequency often seen in Europe and beginning to be utilized in the U.S. The second was a voltage doubler operating at the 915 MHz frequency popular with RF/ID designs in the U.S. Both circuits were designed around Hewlett-Packard's new plastic packaged zero bias Schottky, the HSMS-285X series. To maintain

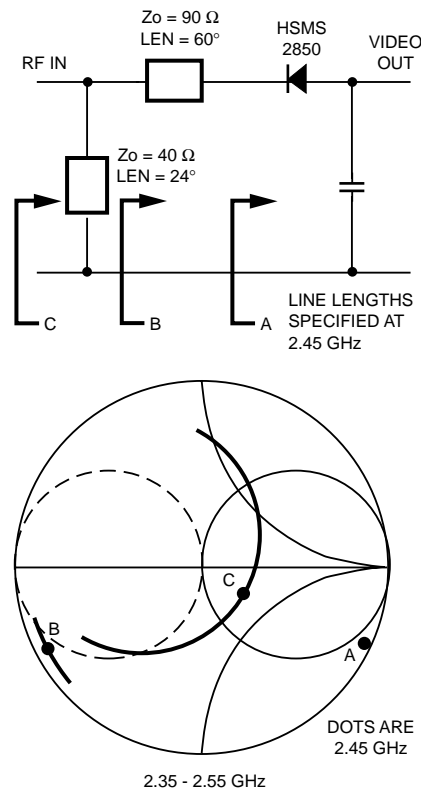


**Figure 19. Design of the 2.45 GHz Detector Matching Network**

generality, both were designed to an input impedance of  $50 \Omega$ .

### Measured Data — 2.45 GHz Single

Using the techniques outlined above, a matching network was designed as shown in Figure 19.

Point A on the Smith chart indicates the diode's impedance over the 200 MHz band specified. A series transmission line rotates the impedance around to the line marked B. A shunt inductor is realized as a shunt shorted stub of length  $< \lambda/4$ , bringing the final circuit impedance up to the line designated C. Since transmission line elements are small at 2.45 GHz, they were chosen over lumped elements in the matching network since they are "free" (an etched circuit board must be pro-

vided in any case).

Two items about the impedances shown in Figure 19 are worth noting. First, as described in the section above, the circuit impedance was set to swing around the origin of the chart, trading midband match for bandwidth. Second, the effect of dispersion can be seen in this chart in that line B is longer than A, and line C is much longer than line B. The addition of a third element to the matching network would have added to the dispersion, which would severely reduce bandwidth.

The network was realized as a microstrip circuit, as shown in Figure 20.

To save space, the capacitor after the diode was chosen to be a lumped element chip, but an etched capacitor (shunt open circuited stub of length  $= \lambda/4$ ) would have served as well.

The circuit was tested, with the results shown in Figure 21. This diagram shows the measured return loss of the circuit, very close to that predicted from Figure 19.

In Figure 22, the 2.3 to 2.7 GHz swept-frequency output voltage of the detector is shown at an input power of  $1 \mu\text{W}$ . Good bandwidth is achieved for output voltages over 30 mV, resulting in a design which is tolerant of lot-to-lot variations in diode and circuit board characteristics.

Finally, the transfer curve of the diode was measured at 2.45 GHz, as shown in Figure 23.

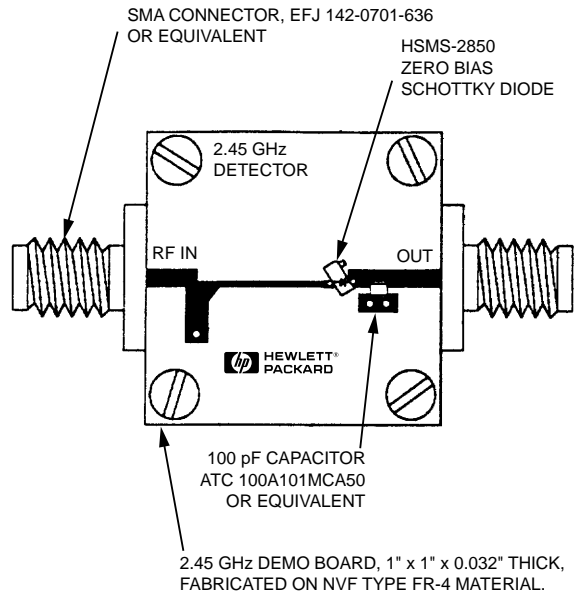


**Figure 20. Physical Realization of the 2.45 GHz Detector**

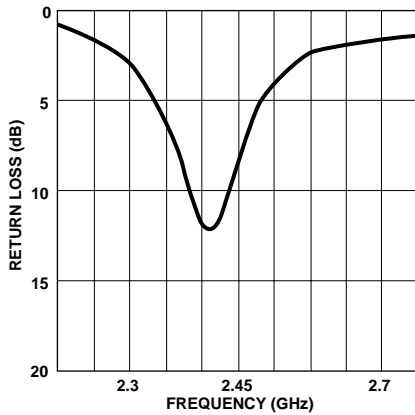


**Figure 21. Measured Input Return Loss ( $P_{in} = -30$  dBm)**

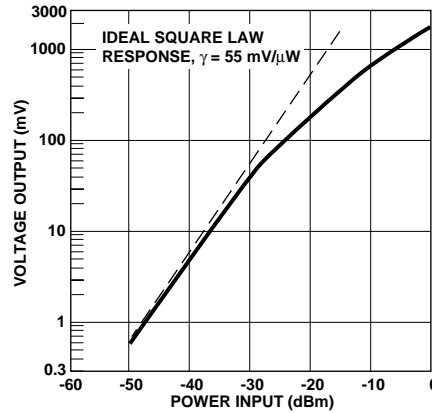


**Figure 23. Measured Transfer Curve for the 2.45 GHz Detector**

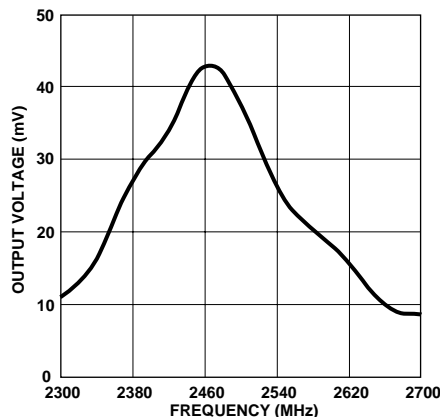


**Figure 22. Measured Output Voltage ( $P_{in} = -30$  dBm)**

Measured tangential signal sensitivity or TSS (14) for this detector was -56 dBm with a 2 MHz video bandwidth.

**Measured Data — 915 MHz Doubler**

Using two Schottky diodes as a voltage doubler, as shown in Figure 4, results in a shift in the impedance due to the doubling of the parasitic capacitance. This is illustrated in Figure 24. As a result, the elements of the matching network for the diode pair will be substantially different from those for the single diode.

(14) Agilent Technologies Application Note 956-1, *The Criterion for the Tangential Sensitivity Measurement.*

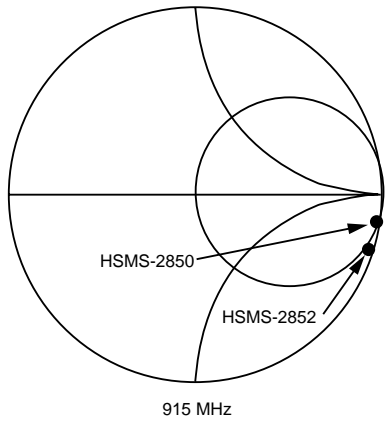


**Figure 24. Impedances of Single and Double Diodes**

The matching network for the doubler is shown in Figure 25.

Because of the excessive size of distributed transmission line matching elements at 915 MHz, lumped elements were chosen for this design. A short section of series line (required to mount the diode) and a 46 nH series inductor rotate the impedance of the diode pair around the Smith chart to the line of constant susceptance which runs through the origin. However, since a shunt inductor or shunt shorted stub cannot be used for the outermost element (to do so would short out the shunt diode), the designer rotates the diode impedance up into the inductive half of the chart to the point marked **B**. From this point, a shunt capacitor (or a shunt open circuited stub) can bring the impedance down to the origin. The shunt capacitor was adjusted to keep point **C** just above the origin so as to obtain better bandwidth with a small sacrifice in midband match.

The circuit was realized as shown in Figure 26, with all parts soldered to an FR4 microstrip board of 0.032" thickness. In addition to the circuit elements shown in

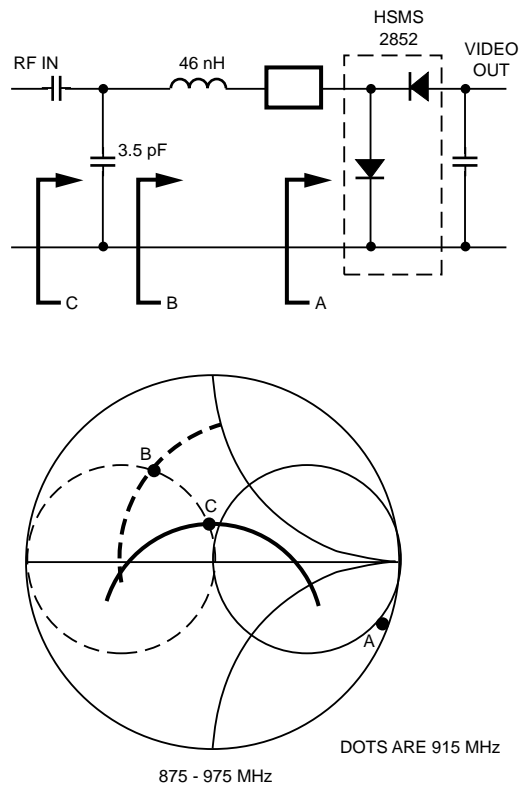


**Figure 25. Design of the 915 MHz Doubler Matching Network**

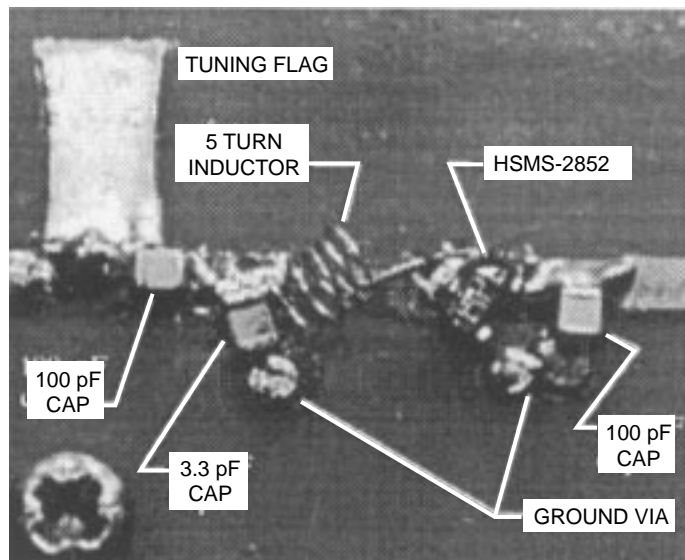


**Figure 26. Photograph of the Voltage Doubler**



Figure 25, a small tuning flag (shunt capacitance) was added at the detector input to optimize performance. It contributed approximately 10% to the output voltage.

Figure 27 shows the measured return loss of the prototype circuit, once again illustrating the good bandwidth which can be obtained by giving up a bit of midband match. Vertical scale is 5 dB/division.

A 850 to 950 MHz swept measurement of output voltage was made with an input power of  $1 \mu\text{W}$ , as shown in Figure 28. Vertical scale is 10 mV/division, and the horizontal scale is 10 MHz/division.

At 915 MHz, the transfer curve of the doubler was measured, as shown in Figure 29.

In Figures 28 and 29, the very high output voltage of the doubler circuit is illustrated. At midband, more than 65 mV is obtained for a  $1 \mu\text{W}$  input, almost double the 35 mV which can be expected from a single diode detector.

Replacing the shunt capacitor with a higher-Q shunt open circuited stub would have resulted in a slight increase in output voltage, but at the cost of increased circuit size.

## Conclusions

The Schottky diode crystal video receiver has been shown to be a cost effective and power saving

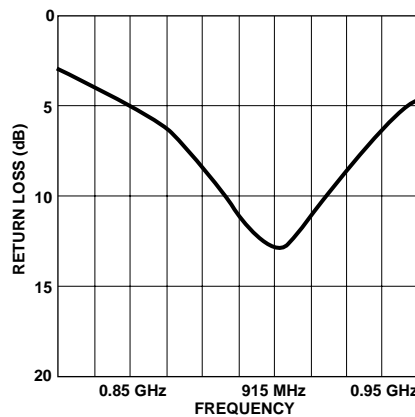


Figure 27. Measured Return Loss at  $P_{in} = -30 \text{ dBm}$

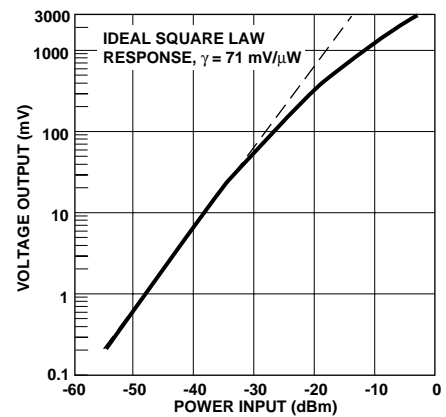


Figure 29. Measured Transfer Curve

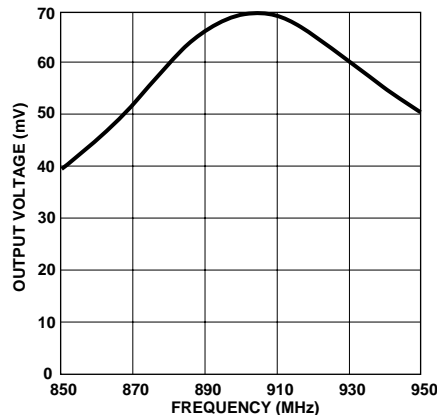


Figure 28. Measured Output Voltage with  $P_{in} = -30 \text{ dBm}$

alternative to the superheterodyne receiver for RF/ID tags. Methods for the design of Schottky diode RF/ID detectors have been described, and measured data from two practical examples have been given.